

WEDNESDAY SLIDE CONFERENCE  
2020-2021

Conference 22

14 April, 2021



Joint Pathology Center  
Silver Spring, Maryland

---

**CASE 1: 20-003333 (4155466-00)**

**Signalment:**

8 month old, male-intact, Huacaya, *Vicugna pacos*, alpaca

**History:**

The cria presented for a simple, closed, spiral fracture of the distal left humerus which was repaired with surgical intervention. Following surgery, the cria was severely hypoglycemic and seizing. Despite intensive therapy, the cria died a few days later.

**Gross Pathology:**

The alpaca presented to necropsy with a body condition score of 1/5. The fiber of the cria was black. The diaphysis of the left humerus was fractured without obvious formation of a fibrous callus and held in place with a metal plate. The cortical bone of the left humerus thin to segmentally non-discernable. The humeral fascia and skeletal muscles, extending to the proximal humerus to just distal the cubital joint, were edematous and hemorrhagic. Many transverse fractures with hard, bony fracture calluses were through the mid bodies of the right 5th – 10th ribs. Subjectively, the ribs were easily broken. On longitudinal section of the left femur, the proximal physis was irregularly thickened. The epicardial fat was clear and gelatinous (serous atrophy).



Proximal humerus, alpaca. The cortical bone of the left humerus markedly thinned. There is a screw hole within the metaphysis due to previous attempts at fracture repair. (Photo courtesy of: Auburn University - Department of Pathobiology <https://www.vetmed.auburn.edu/academic-departments/dept-of-pathobiology/>)



Thoracic plate, alpaca: Ribs 4-10 exhibit calluses from diaphyseal fracture. (Photo courtesy of: Auburn University - Department of Pathobiology <https://www.vetmed.auburn.edu/academic-departments/dept-of-pathobiology/>)

### Laboratory results:

A serum biochemistry was performed the day of death. Reference intervals are based on values published by UC Davis Veterinary Medical Teaching Hospital.<sup>8</sup>

SDH: 52.1 U/L (reference interval [RI]: 2 – 5)

AST: 3249 U/L (RI: 107 - 199)

CK2: 13405 U/L (RI: 37 – 108)

Total bilirubin: 0.36 mg/dL (RI: 0.0 – 0.1)

BUN: 39.9 mg/dL (RI: 7 – 22)

Calcium: 8.4 mg/dL (RI: 9.0 – 9.9)

Phosphorous: 5.9 mg/dL (RI: 4.3 – 8.3)

### Microscopic description:

Left proximal humerus: The segmentally and irregularly thickened physal cartilage has persistent tongues and disorganized clusters of hypertrophic, degenerate and necrotic chondrocytes that extend into the ill-defined primary and secondary spongiosa. The slender and frequently fragmented trabecular bony spicules have central cartilage, surrounded by woven and lamellar bone. The intertrabecular space is composed of a loose fibrovascular meshwork with intermixed rare, mature adipocytes and predominately later-stage hematopoietic elements. The metaphyseal cortex is flared, and the markedly attenuated to absent cortical bone is covered by an approximately 150 µm thick layer of fibrous periosteum. A focus of moderate hemorrhage is within the periosteum and the adjacent endomysium and perimysium. A cleft in the proximal diaphysis (previous location

of screw) is surrounded by hemorrhage and displaces the bony spicules to the periphery.

### Contributor's morphologic diagnosis:

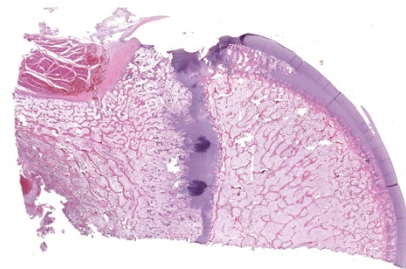
Left proximal humerus: Physal chondrodystrophy and delayed endochondral ossification (rickets).

Left proximal humerus: Fibrous osteodystrophy with osteopenia.

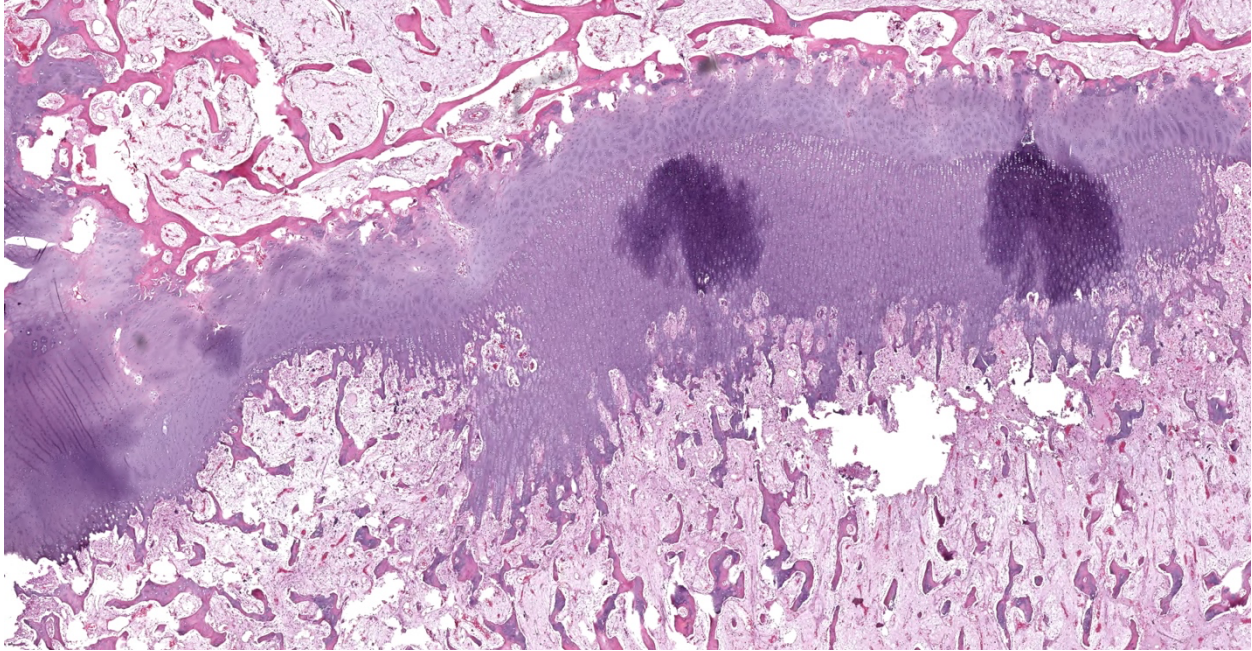
### Contributor's comment:

Randomly distributed, moderate, neutrophilic acute hepatitis and minimal, acute, neutrophilic, interstitial pneumonia were diagnosed with histological examination of the standard tissues. These findings, along with the history of profound hypoglycemia, pointing to likely peracute septicemia as the cause of death. The emaciation (supported by a poor body condition and serous atrophy of epicardial fat) is considered to be a contributing cause of death for this case leading to an inability to mount a sufficient immune response.

Ultraviolet B dermal radiation converts 7-dehydrocholesterol (7-DHC) to pre-vitamin D<sub>3</sub> in keratinocytes, which then undergoes thermal isomerization to vitamin D<sub>3</sub>. Vitamin D<sub>3</sub>, as well as dietary vitamin D<sub>2</sub>, are bound to vitamin D-binding protein and transported to the liver. In the liver, hepatic cytochrome 450 enzymes (such as CYP27A1, CYP3A4, CYP2R1, and CYP2J3) carry out 25-hydroxylation of vitamin D, converting it to 25-hydroxyvitamin D. Under the tight regulation of parathyroid hormone and



Proximal humerus, alpaca. At subgross magnification, the physis is irregular and there are segmental areas of retained cartilage projecting into the metaphysis. A screw hole from a prior attempt at fracture fixation is present at the diaphyseal edge and secondary spongiosa is remodeled concentrically around it. (HE, 5X)



*Proximal humerus, alpaca. The physis is irregularly thickened by tongues of unremodeled cartilage extending downward into the metaphysis. Hematopoietic cells are absent and intratrabecular spaces are filled with loosely arrange fibrous connective tissue. Focal dark staining of physeal cartilage is artifactual. (HE, 19X)*

plasma phosphorous, the kidney produces either the most active form of vitamin D, 1,25-dihydroxyvitamin D, or the inert metabolites, 24,25-dihydroxyvitamin D or 1,24,25-trihydroxyvitamin D.<sup>1,2</sup>

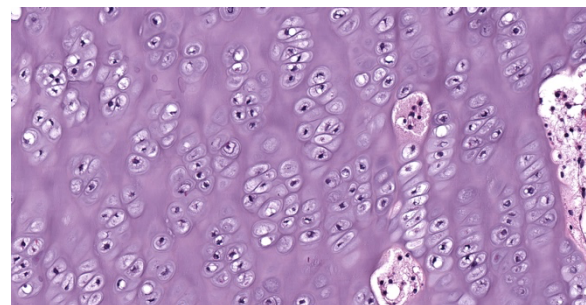
Melanin in the skin competes with 7-DHC for ultraviolet photons, so animals with pigmented skin require more UVB exposure for previtamin D<sub>3</sub> formation. Animals at higher altitudes are exposed to higher levels of UVB and, therefore, may not need prolonged exposure to the sun for sufficient previtamin D<sub>3</sub>.<sup>2</sup>

Vitamin D targets, indirectly or directly, the kidneys, parathyroid glands, intestine, and bone. In the intestine, vitamin D promotes the uptake of calcium and increase active phosphate absorption. Transient receptor potential vallinoid 6 (TRPV6) transports calcium into the intestinal enterocyte to bind to calbindin D. Calbindin D transports calcium to PMCA1b and NCX1 to excrete calcium into the bloodstream. Both TRPV6 and calbindin D are upregulated by vitamin D.<sup>2</sup>

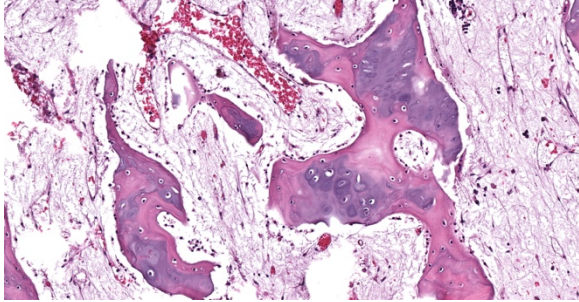
Vitamin D maintains the ionized blood calcium concentration by mobilizing calcium from bone

stores. Vitamin D likely stimulates RANKL, thereby increasing binding to RANK on osteoclasts and stimulates the maturation of osteoclast progenitor cells to osteoclasts (osteoclastogenesis). The decoy receptor osteoprotegerin (OPG) is downregulated by vitamin D. Binding of RANLK to OPG inhibits osteoclastogenesis.

Vitamin D is partially balanced by parathyroid hormone. Vitamin D deficiencies result in hypocalcemia, stimulating the parathyroid gland to secrete parathyroid hormone. Excess vitamin D can suppress the parathyroid gland by



*Proximal humerus, alpaca. Chondrocytes in the hypertrophic zones in retained cartilage lose their vertical orientation, forming disordered chondrones and impairing vascular invasion. (HE, 334X)*



*Proximal humerus, alpaca. Metaphyseal trabeculae have wide osteoid seams, dense cartilaginous cores, and few lining osteoclasts indicating active remodeling. Hematopoietic precursors are sparse. (HE, 118X)*

decreasing growth factors, inhibit cell growth, and increasing ionized calcium sensitivity of the parathyroid gland.<sup>2</sup>

Black-coated alpacas are predisposed to developing vitamin D deficiency. Previous research has demonstrated that black-coated alpacas have lower serum vitamin D<sub>3</sub> all year, with vitamin D<sub>3</sub> levels that do not fluctuate with yearly solar radiation levels, unlike lighter-coated alpacas.<sup>6</sup> Bone density in light-coated alpacas, along with serum vitamin D<sub>3</sub> and phosphorous concentrations, does fluctuate with, but lags behind, seasonal levels of solar radiation. Due to this lag, the nadir of bone density and vitamin D<sub>3</sub> in the northern hemisphere is from January to May despite solar irradiation being lowest in December.<sup>5</sup>

Rickets is a disease in immature and growing animals, such as in this case of an 8-month-old animal, caused by a deficiency in vitamin D and/or phosphorous. Affected animals with rickets will fail to mineralize their bone and have subsequent deformities, pathological fractures, and bone pain. In rickets, this failure of mineralization and endochondral ossification causes the growth plates to be irregularly thickened. This thickening of the growth plates is especially prominent in the costochondral junctions, forming a row of nodular thickenings – classically termed ‘rachitic rosary’ due to the string of beads-like appearance.<sup>4</sup>

Vitamin D deficiency histologically differs from phosphorous deficiency rickets in bone. Both forms will develop the characteristic physéal

failure of endochondral ossification. However, lack of vitamin D impairs the absorption of calcium from the intestine and the reabsorption of calcium from bone, leading to hypocalcemia and secondary hyperparathyroidism. Because of the hypocalcemia, younger animals with vitamin D deficiency have lesions that overlap with rickets and fibrous osteodystrophy.<sup>1</sup> This is most notable in the cortical and trabecular bone. With phosphorous deficiency, the trabecular and cortical bone contains excess unmineralized osteoid leading to failed osteoclast resorption and impaired bone modeling/remodeling. With vitamin D deficiency, there is extensive resorption and replacement of the trabecular and cortical bone with fibrous connective tissue (features of fibrous osteodystrophy).<sup>4</sup>

#### **Contributing Institution:**

Auburn University - Department of Pathobiology  
<https://www.vetmed.auburn.edu/academic-departments/dept-of-pathobiology/>

#### **JPC diagnosis:**

1. Long bone: Physéal and epiphyseal osteodysplasia, diffuse, with regional delayed endochondral ossification (rickets).
2. Long bone: Osteopenia, trabecular and cortical, diffuse.
3. Long bone: Serosus atrophy of fat, diffuse, marked.

#### **JPC comment:**

The moderator emphasized that these lesions may be due, in part, to rickets. Other portions of the bone, such as the fewer and thinner bony trabeculae, are features of osteopenia. The clinical history and gross findings may also support malnourishment in this animal, contributing to the lesions observed in this animal. The moderator described three features likely occurring concurrently in this animal: fibrous osteodystrophy, delayed endochondral ossification, and chondrodystrophy. Contributing factors may have been protein and caloric restriction, hypocalcemia, and vitamin D deficiency.

Vitamin D balance is crucial for calcium and phosphorus homeostasis, and its deficiencies are

well illustrated by this case. Different species depend on vitamin D for this balance to different degrees, and it has been hypothesized that these differences can be attributed to evolutionary adaptation to different environments. The movement of animal life from aquatic environments, which is relatively higher in calcium and lower in phosphorus than land environments, necessitated new mechanisms to absorb calcium and regulate the balance with phosphorus needs. Successful adaptations included the increased absorption of calcium from the gastrointestinal system, more flexible bone remodeling which acts as a calcium reservoir, and the maturation of three intertwined hormones that regulate the calcium and phosphorus balance. Parathyroid hormone, vitamin D, and fibroblast growth factor 23 (FGF23) all act together to provide feedback to the absorption, reservoir, and elimination mechanisms within the body to provide an optimum balance for life.<sup>7</sup>

While the effects of PTH and vitamin D are regularly described and detailed, FGF23 is more recently characterized. FGF23 is secreted by osteoblasts and osteocytes when stimulated by 1,25(OH)<sub>2</sub>D<sub>3</sub>, PTH, or chronically elevated levels of serum calcium and phosphorus. The elaboration of FGF23 provides negative feedback to PTH secretion, inhibits renal absorption of phosphorus, and reduces the capacity of the kidney to activate vitamin D.<sup>7</sup>

The moderator emphasized that FGF23 sits at an interesting intersection of rickets and fibrous osteodystrophy/osteopenia, providing critical feedback to the systems regulating these processes. In this case, it is not immediately clear whether FGF23 is implicated in the development of disease, or might be a useful target for therapy.

Defects in renal 1- $\alpha$ -hydroxylase results in vitamin D-dependent rickets, Type 1, where 25(OH)D<sub>3</sub> cannot be transformed to 1,25(OH)<sub>2</sub>D<sub>3</sub>. This key enzyme is encoded by the gene *CYP27B1* (type 1a), or *CYP27R1* (type 1b), and mutations have been documented as autosomal recessive disease in humans, Hannover pigs, a few cats, and one Saint Bernard dog.<sup>1</sup> This disease manifestation in cats is due to

mutated *CYP27B1* genes, but there have been different mutation locations and types, indicating non-specific initiating events. Additional research may focus on interactions in non-coding regions supporting these exons.<sup>3</sup>

#### References:

1. Craig LE, Dittmer KE, Thompson KG. Bones and Joints. In: Vol. 1, *Jubb, Kennedy & Palmer's Pathology of Domestic Animals: Volume 1*. Elsevier; 2016:16-163.e1.
2. Dittmer KE, Thompson KG. Vitamin D Metabolism and Rickets in Domestic Animals. *Vet Pathol*. 2011 Mar 15;48:389-407.
3. Grahn RA, Ellis MR, Grahn JC, Lyons LA. A novel *CYP27B1* mutation causes a feline vitamin D-dependent rickets type Ia. *J Feline Med Surg*. 2012;14(8):587-590.
4. Olson EJ, Carlson CS. Bones, Joints, Tendons, and Ligaments. In: Zachary JF, ed. *Pathologic Basis of Veterinary Disease*. St. Louis: Elsevier; 2017:954-1008.e2.
5. Parker JE, Timm KI, Smith BB, et al. Seasonal interaction of serum vitamin D concentration and bone density in alpacas. *Am J Vet Res*. 2002 Jul;63:948-953.
6. Smith BB, Van Saun RJ. Seasonal changes in serum calcium, phosphorus, and vitamin D concentrations in llamas and alpacas. *Am J Vet Res*. 2001 Aug;62:1187-1193.
7. Uhl EW. The pathology of vitamin D deficiency in domesticated animals: An evolutionary and comparative overview. *International Journal of Paleopathology*. 2018; 23:100-109.
8. Veterinary Medical Teaching Hospital - University of California Davis. Clinical Chemistry Reference Intervals. 2010.

---

#### **CASE 2: MW19-0351 (4152807-00)**

##### **Signalment:**

6 year old, male castrated, Arabian cross, *Equus caballus*, equine

##### **History:**

A 6-year-old Arabian gelding presented initially with a history of reduced appetite, and low-grade fever. CBC revealed anemia and leukopenia and chemistry revealed azotemia, hypoglobulinemia,



*Kidney, horse. Approximately 95% of the parenchyma and of the left kidney and 25% of the right kidney is effaced by a soft, tan mass. (Photo courtesy of: Midwestern University College of Veterinary Medicine, Diagnostic Pathology Center, 5725 West Utopia Rd., Glendale, AZ 85308 <https://www.mwuanimalhealth.com/diagnostic-pathology-center/>)*

hyperphosphatemia and hyperkalemia. Urinalysis was in the isosthenuric range indicating renal failure. Ultimately, the patient became depressed and tachycardic, and then had a neurologic episode that consisted of seizure, recumbency, nystagmus from which he never recovered. Due to the poor prognosis, euthanasia was elected.

### **Gross Pathology:**

The carcass was in fair body condition and good postmortem condition. The left kidney was severely enlarged, weighing 7.15 kg. On cross section, approximately 95% of the renal parenchyma of the left kidney is effaced by a soft, yellow to tan mass. Similarly, there is a soft, yellow to tan, peripherally expansile, spherical mass obliterating approximately 20% of the renal parenchyma of the right kidney. Three lymph nodes were enlarged in the immediate vicinity of the right kidney and adrenal gland. These lymph nodes ranged in size from 2.5 cm to 3.5 cm in diameter and on cut section, the corticomedullary

distinction was completely obscured by firm, tan, soft, tan to white, variably sized (4-7 mm in diameter) coalescing nodules. The brain was grossly unremarkable.

### **Laboratory results:**

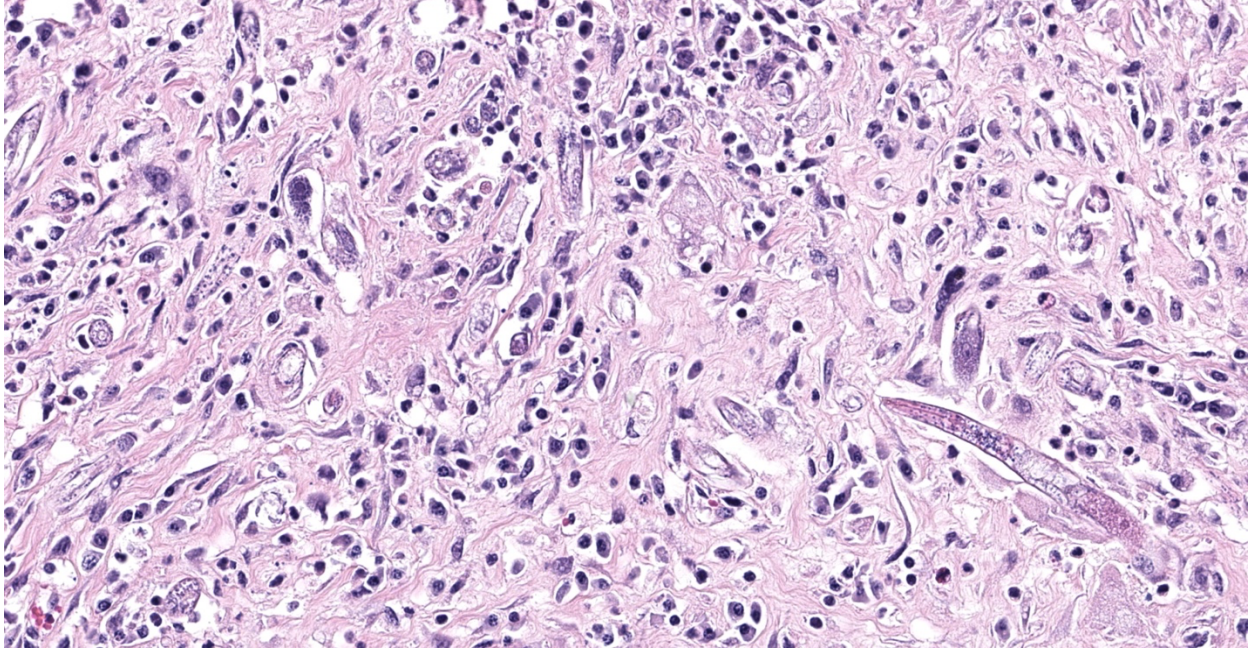
No additional testing performed

### **Microscopic description:**

Obliterating approximately 90% of the renal parenchyma within the section are multifocal to coalescing, variably sized, moderately to densely cellular aggregates of inflammatory cells composed predominately of epithelioid macrophages that are often multinucleated (Langhans-type) admixed with moderate numbers of lymphocytes and plasma cells and fewer eosinophils separated by abundant, variably mature, fibrous connective tissue. The described inflammatory cells are variably centered on and around large numbers of randomly distributed, tangential and cross-sections of adult and larval nematodes as well as numerous nematode eggs. The adult nematodes are approximately 15-20 microns in diameter and up to 300-400 microns in length, and have a thin cuticle, platymyarian-meromyarian musculature, intestinal tract, and characteristic rhabditiform esophagus with a corpus, isthmus and terminal bulb. A uterus containing a dorsoflexed ovary is also occasionally identified within the adult nematodes. Larval nematodes are also present and typically measure 10-15 microns in diameter and 150-250 microns in length and have the characteristic rhabditiform esophagus. Parasitic eggs are 10 x 25-40 microns, ovoid, and both embryonated and larvated.



*Kidney, horse. A single section of kidney (capsule at left) is submitted for examination. 80% of the cortex and medulla in this section are effaced by multifocal to coalescing areas of granulomatous inflammation. (HE, 5X)*



*Kidney, horse. Areas of granulomatous inflammation contain variable combinations and concentrations of macrophages (uni- and multinucleated), lymphocytes, and plasma cells on moderately dense fibrous matrix. There are numerous cross and tangential sections of larval nematodes and a cross section of an adult female with a prominent esophagus (lower right). (HE, 380X)*

**Contributor’s morphologic diagnosis:**

Kidney: Nephritis, granulomatous, lymphoplasmacytic, multifocal to coalescing, severe, with myriad intralesional rhabditoid nematode adults, larvae, and eggs, etiology presumptive *Halicephalobus gingivalis*

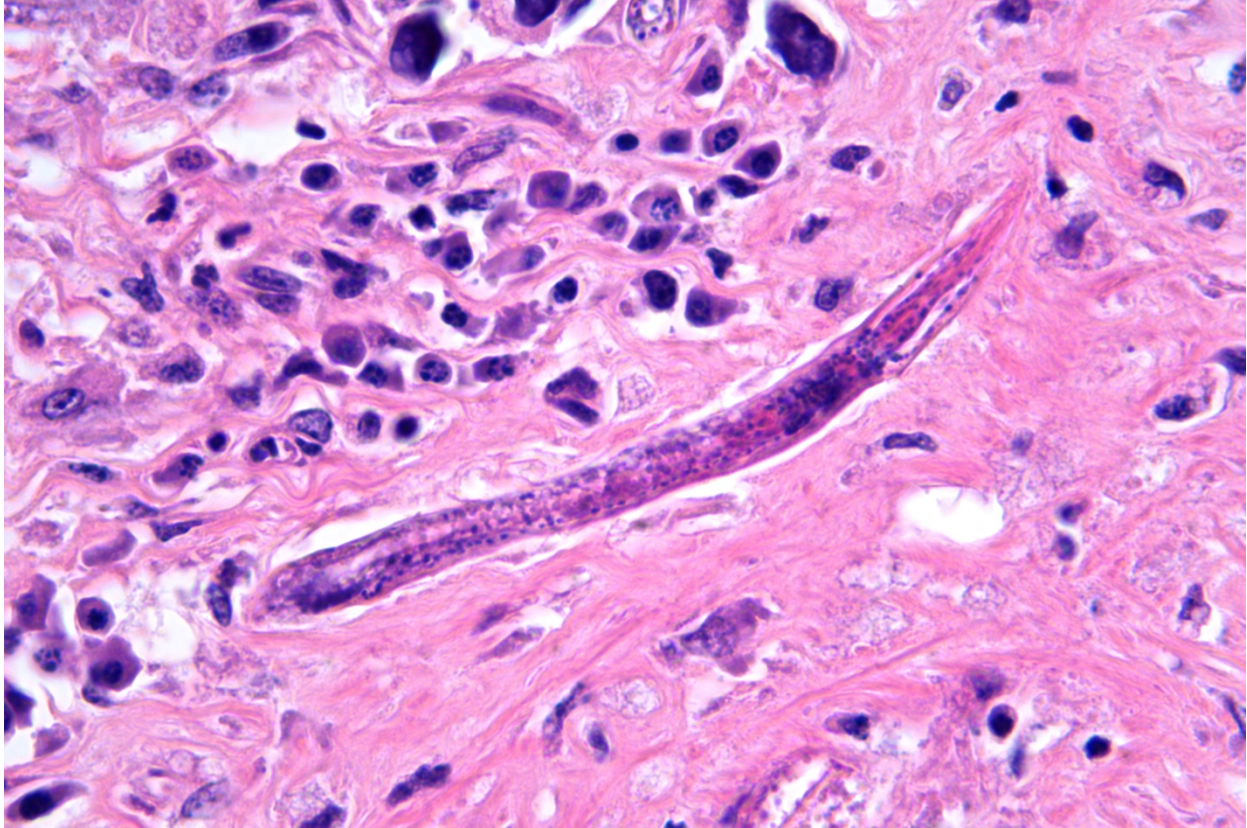
**Contributor’s comment:**

In addition to nephritis, microscopic examination of the brain and lymph node from this horse identified both meningoencephalitis and lymphadenitis with intralesional rhabditoid nematodes that were consistent with *Halicephalobus gingivalis*.

*Halicephalobus gingivalis* is a facultative, opportunistic nematode of the order *Rhabditida*, family *Panagrolaimidae*. The life cycle and pathogenesis of this opportunistic pathogen is still poorly understood. *Halicephalobus* nematodes are found free-living in association with water, soil, and decaying organic matter and it is thought that transmission occurs primarily via wounds in the skin or mucous membranes.<sup>7,9</sup> Rarely, other routes of infections have been suggested, including transmammary.<sup>12</sup> Upon infection, dissemination of the infection is then

thought to occur hematogenously.<sup>6</sup> Although both males and females exist in the environment, only female nematodes have been observed within microscopic lesions, suggesting that within a host, reproduction occurs asexually via parthenogenesis.<sup>7,9</sup>

In veterinary species, this parasitic infection is considered uncommon and sporadic, however when described, has been most commonly reported in horses. To date, only a single case series of *H. gingivalis* infection in cattle has been published.<sup>4</sup> Cases in domestic horses have been identified worldwide, including the Southwestern United States, which is where this horse originated (specifically was from New Mexico). The most commonly reported sites of infection in horses are the brain, kidneys, lymph nodes, oral and nasal mucosa, and adrenal glands.<sup>3,6,7,11</sup> Very rare cases of meningoencephalitis and myelitis associated with *H. gingivalis* infection have been described in humans.<sup>9-10</sup>



Colon, foal. Adult female *Halicephalobus gingivalis* have a prominent tripartite esophagus with a corpus, isthmus, and bulb. (HE, 400X). (Photo courtesy of: Midwestern University College of Veterinary Medicine, Diagnostic Pathology Center, 5725 West Utopia Rd., Glendale, AZ 85308 <https://www.mwuanimalhealth.com/diagnostic-pathology-center/>)

**Contributing Institution:**

Midwestern University College of Veterinary Medicine  
Diagnostic Pathology Center  
<https://www.mwuanimalhealth.com/diagnostic-pathology-center>

**JPC diagnosis:**

Kidney: Nephritis, granulomatous, chronic, focally extensive, severe, with adult and larval rhabditid nematodes and eggs.

**JPC comment:**

This rhabditoid nematode was previously known as *Micronema deletrix*, and while primarily affecting equids, it has been described in other species as well. Numerous cases of fatal encephalitides have occurred in humans<sup>8</sup> and horses, with several cases observing larva in CSF fluid collected either antemortem or postmortem. The migrating larva induced a sterile neutrophilic and mononuclear pleocytosis.<sup>1</sup>

These are free living nematodes, that thrive in soil, compost, manure, even deep within the core of the Earth. A facultative parasite, it infects horses more frequently than humans, and even less frequently cattle. In cases where disseminated disease occurs, they may be seen in kidneys, the brain or spinal cord, lymph nodes, oronasal mucosa, adrenal glands, the heart, and even bone (mandibular and maxillary infections reported).

Descriptive features of *H. gingivalis* include a diameter of approximately 15-25µm, a smooth cuticle, platymarian-meromyarian musculature, a rhabditiform esophagus composed of a corpus, isthmus, and bulb, a gastrointestinal tract lined by uninucleate cuboidal cells, and a single genital tract. Within well-developed lesions, tangential and cross sections of adults as well as larva are easily visualized, with intermixed 10-15µm diameter, ovoid, embryonated eggs.<sup>5</sup>

From its first description in a nasal swelling of a horse in 1965, it has enjoyed broad spread across the world into diverse environments. Cases of *H. gingivalis* infection in horses have been reported in the United States, Canada, Brazil, the United Kingdom, France, Austria, and Turkey. The nematode's ability to survive in varied environmental conditions allows infection of horses, and humans in infrequent cases.<sup>2</sup>

#### References:

1. Adedeji AO, Borjesson DL, Kozikowski-Nicholas TA, Cartoceti AN, Prutton J, Aleman M. What is your diagnosis? Cerebrospinal fluid from a horse. *Veterinary Clinical Pathology*. 2015;44(1):171-172.
2. Bowman DD. *Georgis' Parasitology for Veterinarians*, 10<sup>th</sup> Ed. St. Louis, MO:Elsevier. 2014;191-192.
3. Bryant UK, et al. *Halicephalobus gingivalis*-associated meningoencephalitis in a Thoroughbred foal. *J Vet Diagn Invest*. 2006; 18:612-615.
4. Enemark HL et al. An outbreak of bovine meningoencephalomyelitis with identification of *Halicephalobus gingivalis*. *Vet Parasitol*. 2016;218-82-86.
5. Gardiner CH, Poynton SL. Morphologic characteristics of rhabditoids in tissue section. In: *An Atlas of Metazoan Parasites in Animal Tissues*. Washington DC, AFIP Press, pp. 14-16.
6. Henneke C et al. The distribution pattern of *Halicephalobus gingivalis* in a horse is suggestive of a haemotogenous spread of the nematode. *Acta Vet Scand* 2014; 56:1-4.
7. Hermosilla C et al. Fatal equine meningoencephalitis in the United Kingdom caused by the panagrolamid nematode *Halicephalobus gingivalis*: case report and review of the literature. *Eq Vet J*. 2011; 43: 759-763.
8. Lim CK, Crawford A, Moore CV, et al. First human case of fatal *Halicephalobus gingivalis* meningoencephalitis in Australia. *Journal of Clinical Microbiology*. 2015;53:1768-1774.
9. Onyiche TE et al. Parasitic and zoonotic meningoencephalitis in humans and equids: Current knowledge and the role of *Halicephalobus gingivalis*. *Parasite Epidemiol Control*. 2018; 3(1): 36-42.
10. Papadi B et al. *Halicephalobus gingivalis*: A rare cause of meningoencephalomyelitis in

humans. *Am J Trop Med Hyg* 2013; 88(6): 1062-4.

11. Wilkins PA, et al. Evidence of *Halicephalobus delatrix* (*H. gingivalis*) from dam to foal. *J Vet Intern Med*. 2001;15:412-417.

---

#### CASE 3: N19-187 (4152932-00)

##### Signalment:

Adult male Virginia opossum (*Didelphis virginiana*)

##### History:

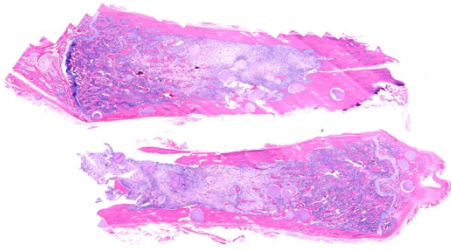
The patient was a wild opossum and presented to the wildlife clinic by a concerned member of the community for ill-thrift. On physical examination, the patient was severely dehydrated and emaciated. On full body radiographs, numerous radiolucent, pinpoint foci were identified throughout all bones in the axial and appendicular skeleton (Radiograph 1; Radiograph 2). The patient was euthanized due to poor prognosis.

##### Gross Pathology:

On gross postmortem examination, the patient was severely emaciated and dehydrated. The pericardial and bone marrow pericardial adipose were translucent, gelatinous, and pale yellow (serous atrophy of fat). Randomly distributed



Presentation, opossum. Scattered throughout the skeletal muscle, there are numerous 1mm apicomplexan cysts. (Photo courtesy of: Cummings School of Veterinary Medicine at Tufts University, Pathology department, 200 Westboro Rd, North Grafton, MA 01536, <https://vetmed.tufts.edu/pathology-service/>)



Long bones, opossum. Two sections of a long bone (presumptively distal ulna) are submitted for examination. At subgross magnification, apicomplexan cysts are visible both within the marrow cavity, as well as within cortical Haversian canals. (HE, 5X)

throughout the skeletal muscle, visceral organs, axial and appendicular skeleton, eyes, and within the lumen of large veins were thousands of pinpoint, spherical, firm, off-white foci.

The stomach was void of ingesta, but contained 30 to 40 round, off-white, 1.25 cm long and 0.1 cm in diameter nematodes with tapered ends.

**Laboratory results:**

None.

**Microscopic description:**

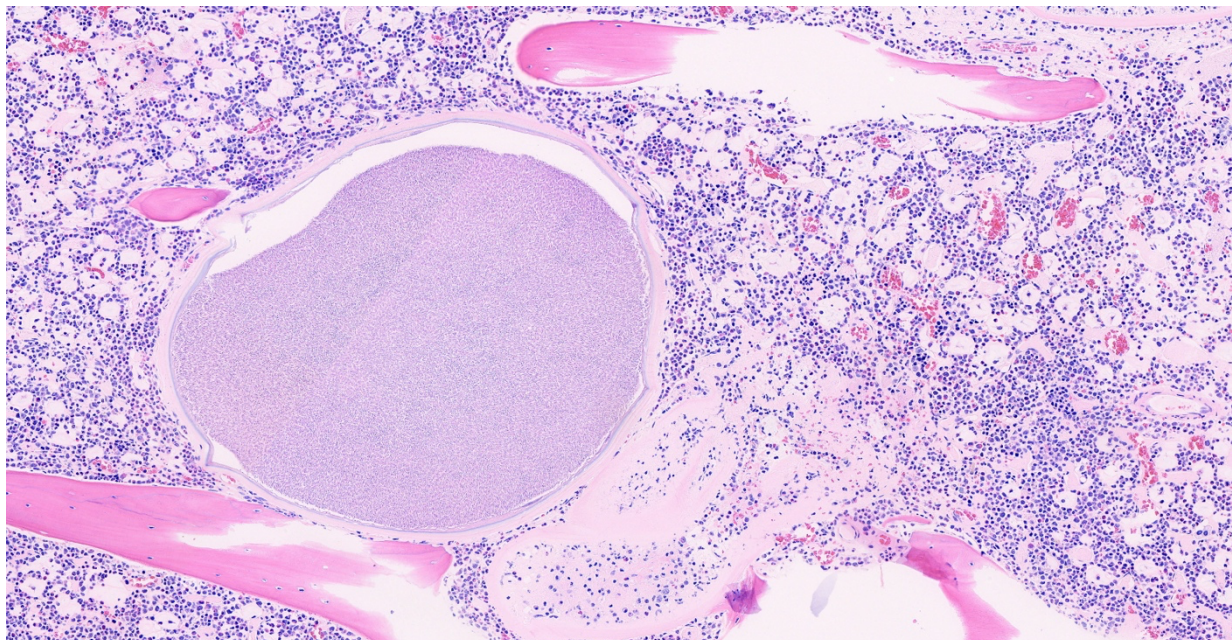
Long bone: Randomly distributed throughout the cortical bone, and within the medullary cavity,

are numerous, round, protozoal cysts, ranging in size from 120 to 300 um in diameter. The cyst wall is 15 µm wide and amphophilic and the cyst contains thousands of spindloid, eosinophilic bradyzoites with a single, basophilic nucleus. A moderate number of cysts are necrotic, characterized by a round lightly eosinophilic structure with a fragmented, discontinuous cyst wall and lack of bradyzoites. Necrotic cysts are encircled by a moderate, dense band of macrophages and degenerate leukocytes that occasionally infiltrate the cyst remnant. The medullary cavity is hypercellular with granulocytic hyperplasia. Bone marrow adipocytes are decreased in number and size and frequently replaced by lightly basophilic, wispy material (serous atrophy of fat).

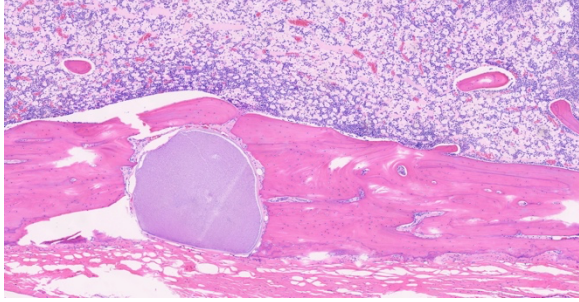
**Contributor’s morphologic diagnosis:**

Long bone, bone marrow: disseminated coccidiosis (consistent with *Besnoitia darlingi* cysts) with marked medullary granulocytic hyperplasia and serous atrophy of fat.

Stomach (not submitted): moderate, focally extensive gastritis with intraluminal nematodes.



Long bone, opossum. Typical *Besnoitia darlingi* schizont with a 10um exterior hyaline capsule, a thin rim of basophilic host cell cytoplasm with multiple nuclei, and numerous small zoites. The collapsed capsule of a necrotic schizont is adjacent at right. (HE, 98X)



Long bone, opossum. *Besnoitia darlingi* schizont within a Haversian canal in the cortex. (HE, 47X)

**Contributor's comment:**

The combination of patient signalment, gross findings, and the morphology of the protozoan cysts were deemed consistent with *Besnoitia* spp, likely *Besnoitia darlingi*. *Besnoitia* are Apicomplexan protozoa, within the *Sarcocystidae* family, and infect a number of wild and domestic mammals, as well as reptiles.<sup>2,7</sup> Felids have been identified experimentally and naturally as the definitive host for a number of *Besnoitia* spp, including *Besnoitia darlingi*.<sup>7,8</sup> Opossums serve as an intermediate host.<sup>5</sup> Diagnosis is based on anatomic lesions, histopathology, immunofluorescence, and electron microscopy.<sup>7</sup>

The pathogenicity of *Besnoitia* is variable and while the underlying causes have not been fully elucidated, young age, immunosuppression, and stress have been suggested as predisposing factors for clinical disease.<sup>2</sup> Infection frequently causes no adverse effects, although animals may have numerous cysts in the skin, striated muscle, and visceral organs.<sup>2</sup> In cattle, *Besnoitia besnoiti* is an economically important disease; in severe infections, it can result in reduced fertility in females and reduced reproductive efficacy in breeding bulls, secondary to orchitis.<sup>3</sup>

In opossums, *Besnoitia darlingi* has historically been considered non-pathogenic, with numerous cysts in the skin, striated muscle and/or visceral organs with lack of an inflammatory response. However, there are reports of severe disease, debilitation, or death.<sup>2</sup> In cattle, immunosuppression has been implicated as a factor in the development of severe cases and skin lesions.<sup>5</sup> Previous reports of disseminated *Besnoitia* in opossums have been associated with immunosuppression in the form of recent

parturition, poor body condition, and gastrointestinal and respiratory parasitism.<sup>5</sup> In this case, the high parasite load may have predisposed the patient to severe emaciation and stress, allowing dissemination of *Besnoitia darlingi*. However, it is difficult to determine if the *Besnoitia* dissemination is cause or effect of emaciation. Another contributing factor was the presence of cysts within the anterior chamber of both eyes, which may have compromised eyesight, making foraging difficult.

**Contributing Institution:**

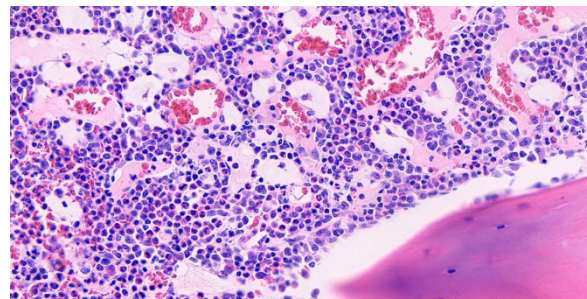
Cummings School of Veterinary Medicine at Tufts University  
 Pathology department  
 200 Westboro Rd  
 North Grafton, MA 01536  
<https://vetmed.tufts.edu/pathology-service/>

**JPC diagnosis:**

1. Long bone, medullary cavity, Haversian canals and periosteum: Apicomplexan cysts, disseminated, with mild granulomatous osteomyelitis.
2. Long bone: Serous atrophy of fat, diffuse, marked.
3. Long bone: Myeloid hyperplasia, diffuse, marked.

**JPC comment:**

The contributor summarizes this entity in opossums concisely. Within the *Besnoitia* genus, species of importance include this *B. darlingi* and *B. tarandi* in opossums, *B. besnoitia* in cattle, *B. bennetti* in donkeys, *B. caprae* in goats, *B. wallacei* in rats, *B. neotomofelis* in woodrats, *B. oryctofelisi* in rabbits, and *B. jellisoni* in mice. As stated by the contributor, for several species for



Long bone, opossum. There is diffuse hyperplasia of the granulocytic compartment of the bone marrow. (HE, 381X)

which the life cycle has been described, the cat is the definitive host, shedding viable oocysts in feces that are morphologically similar to those of *Toxoplasma gondii*.<sup>1</sup>

Despite understanding the life cycle of 4 of the 10 species of *Besnoitia*, the exact mode of transmission remains undetermined. It is currently thought that mechanical transmission by blood-sucking insects is a primary route of transmission, but other routes may exist. In the early stages of disease, tachyzoites in intermediate hosts proliferate in host endothelial cells, monocytes, and neutrophils. As the infection progresses, tissue cysts form, as seen in this case. Each cyst represents a parasitized host cell, with the growing bradyzoites inducing hyperplastic and hypertrophic changes.<sup>6</sup>

The Virginia opossum also has other host adapted parasites that cause little disease in this definitive host. When considering potential disease in horses kept near natural surroundings, it is important to remember that *Didelphis virginiana* is the definitive host for *Sarcocystis falcatula*, and possibly also the definitive host for *S. neurona*. These noble animals are also a reservoir host for *Leishmania brasiliensis*, an important agent that causes human and animal mucocutaneous leishmaniasis.<sup>1,4</sup>

#### References:

1. Bowman DD. *Georgis' Parasitology for Veterinarians*, 10<sup>th</sup> Ed. St. Louis, MO:Elsevier. 2014;109.
2. Ellis, Angela. Debilitation and Mortality Associated with Besnoitiosis. *Journal of Zoo and Wildlife Medicine*. 2012. 43(2): 367-374.
3. Frey, Caroline F., et al. *Besnoitia besnoiti* lytic cycle in vitro and differences in invasion and intracellular proliferation among isolates. *Parasit Vectors*. 2016. 9: 115.
4. Higgins D, Rose K, Spratt D. Monotremes and Marsupials. In: Terio KA, McAloose D, St. Leger J, eds. *Pathology of Wildlife and Zoo Animals*. San Diego, CA:Elsevier. 2018:473-474.
5. L. Diesing. *Besnoitia besnoiti*: studies on the definitive host and experimental infection in cattle
6. Mauldin EA, Peters-Kennedy J. Integumentary System. In: Maxie MG, ed,

*Jubb, Kennedy, and Palmer's Pathology of Domestic Animals*, 6<sup>th</sup> Ed. St. Louis, MO:Elsevier. 2016;661-663.

7. Shaw, Shannon, et. al. *Besnoitia darlingi* infection in a Virginia Opossum (*Didelphis virginiana*). *Journal of Zoo and Wildlife Medicine*. 2009. 40 (1): 220-223.
8. Verma, Shiv. K., et al. Bobcats (*Lynx rufus*) are natural definitive host of *Besnoitia darlingi*. *Veterinary Parasitology*. 2017. 248 (2017): 84-89.

---

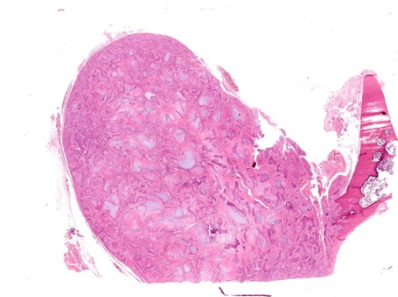
#### CASE 4: 933-17 (4116933-00)

##### Signalment:

14yo female spayed German Shepherd dog (*Canis lupus familiaris*)

##### History:

Presented anorexic for 5 days with polydipsia and intermittent vomiting over the previous week. The animal had lost 3.5kg in the past 3 months. The dog had previously been diagnosed with degenerative joint disease that was being treated with robenacoxib, amantadine, gabapentin, pentosane and fish oil supplementation. On clinical examination, the dog was tachycardiac and tachypneic with harsh lungs sounds. A marked azotemia was noted on a biochemistry profile with moderate elevation in ALT/ALKP (see laboratory results below). The dog was euthanized at the owner's request and submitted for post-mortem examination.



Flat bone, dog. A large polypoid mass composed of repeating lobules of cartilage and bone extends outward from and infiltrates the cortex of the adjacent flat bone. (HE, 5X)

Haematology	Results	Reference Values	
Red cell count x 10 <sup>12</sup> /L	5.6	5.5 – 8.5	
Haemoglobin g/L	137	120 - 180	
Haematocrit L/L	0.38	0.37 – 0.55	
MCV (HCT/RCC)	fL	68	60 - 75
MCH (Hb/RCC)	pg	<b>25</b>	19 - 24
MCHC (Hb/HCT)	g/L	364	320 - 380
RDW-SD	fL	38.8	33.5 – 41.9
Platelets x 10 <sup>9</sup> /L	380	200 - 500	
PDW	fL	<b>9.2</b>	11.1 – 20.8
MPV	fL	<b>8.4</b>	9.8 – 14.0
White cell count x 10 <sup>9</sup> /L	8.1	6.0 – 17.0	
Atypical cells x 10 <sup>9</sup> /L		0	
Bands x 10 <sup>9</sup> /L		0 – 0.3	
Neutrophils x 10 <sup>9</sup> /L	6.6	3.0 – 11.5	
Lymphocytes x 10 <sup>9</sup> /L	1.1	1.0 – 4.8	
Monocytes x 10 <sup>9</sup> /L	0.3	0.2 – 1.4	
Eosinophils x 10 <sup>9</sup> /L	0.1	0.1 – 1.3	
Basophils x 10 <sup>9</sup> /L		< 0.1	
NRBC /100WBC		Rare	
Reticulocytes x 10 <sup>9</sup> /L	16	10 - 110	
Total solids g/L	74	60 - 80	
<b>Comments:</b> None.			
<input type="checkbox"/> Manual differential	<input checked="" type="checkbox"/> Automated differential		

*Hematology results.*

### Gross Pathology:

The lungs were discolored red/purple with a slightly rubbery texture. Both kidneys were irregular in shape with expansion of the renal pelvis and bilaterally the renal papillae were overlaid by friable yellow material. Radiating yellow streaks were present in the renal medullae. Arising from the caudal left parietal and occipital bones of the skull, there was an irregularly shaped, moderately defined, multilobulated, hard mass approximately 6 cm x 4cm x 5cm which protruded from the exterior and interior surface of the skull. The underlying cerebellum was indented at the site of the mass.

### Laboratory results:

See inset tables.

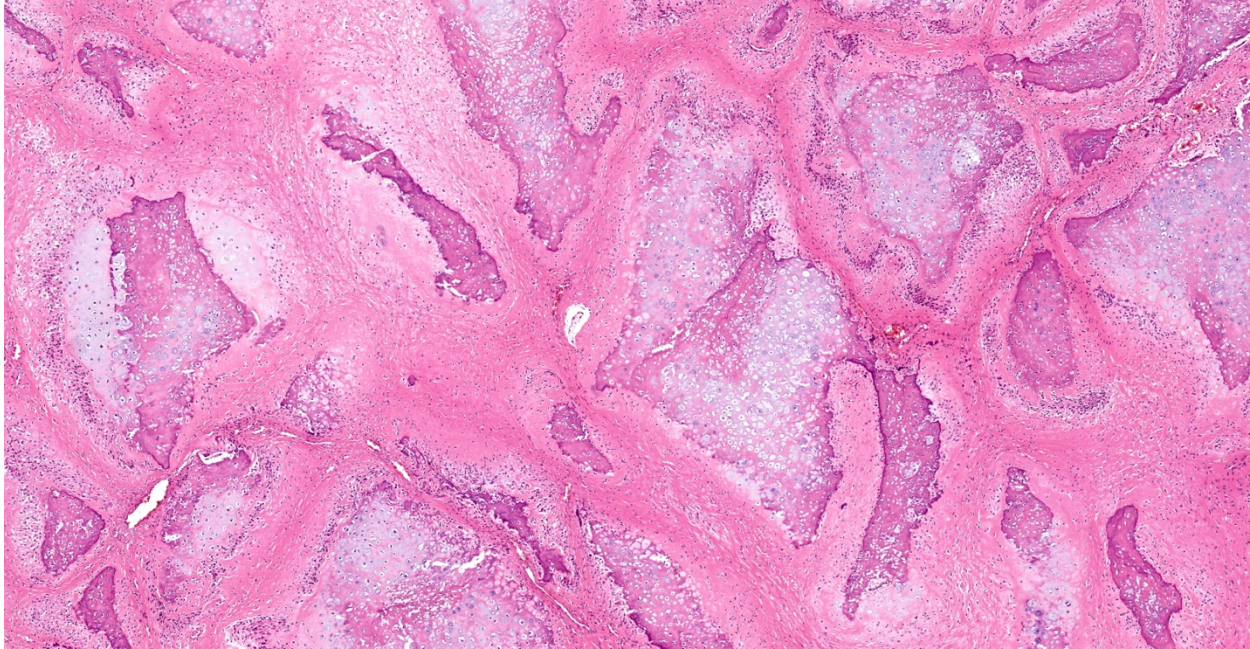
Red cell morphology: Unremarkable.  
White cell morphology: Unremarkable.  
Platelet morphology: Unremarkable.

### Microscopic description:

The mass is composed of irregular islands of hypercellular bone intermixed with a variable quantity of chondroid matrix containing cells within lacunae. Surrounding these islands there is a population of pleomorphic spindle cells which have indistinct margins and lacy chromatin with a single central nucleolus. Occasionally

Biochemistry	Full Profile	Results	Reference Values
Sodium	mmol/L	154	144 - 160
Potassium	mmol/L	4.4	3.5 – 5.8
Chloride	mmol/L	113	109 - 122
Calcium	mmol/L	<b>3.14</b>	2.30 - 3.00
Phosphate	mmol/L	<b>3.1</b>	1.0 – 2.6
Urea	mmol/L	<b>46.8</b>	3.0 – 8.7
Creatinine	µmol/L	<b>585</b>	40 - 140
Glucose	mmol/L	5.5	3.4 – 7.4
Cholesterol	mmol/L	6.0	3.9 – 7.8
Total Bilirubin	µmol/L	2	0 – 20
Conjugated	µmol/L		0 – 5
ALT	U/L	<b>897</b>	3 - 83
ALP	U/L	<b>731</b>	0 - 170
GGT	U/L	3	1 - 12
Amylase	U/L	932	180 - 1200
Lipase	U/L	80	0 - 395
CK	U/L	182	50 - 400
Total protein	g/L	64	55 – 76
Albumin	g/L	36	25 - 40
Globulin	g/L	28	19 - 39
<b>Comments:</b> None.			

*Chemistry results.*



*Flat bone, dog. The neoplasm is composed of numerous islands of cartilage, bone, and spindle cells enmeshed in dense homogenous eosinophilic matrix. (HE, 43X)*

there are giant cells within the population, but mitoses are rare. Dissecting between these regions there are septae of dense fibrous connective tissue. There is complete and active lysis of the adjacent calvarium, but the mass is well-circumscribed with no evidence of invasion.

**Contributor's morphologic diagnosis:**

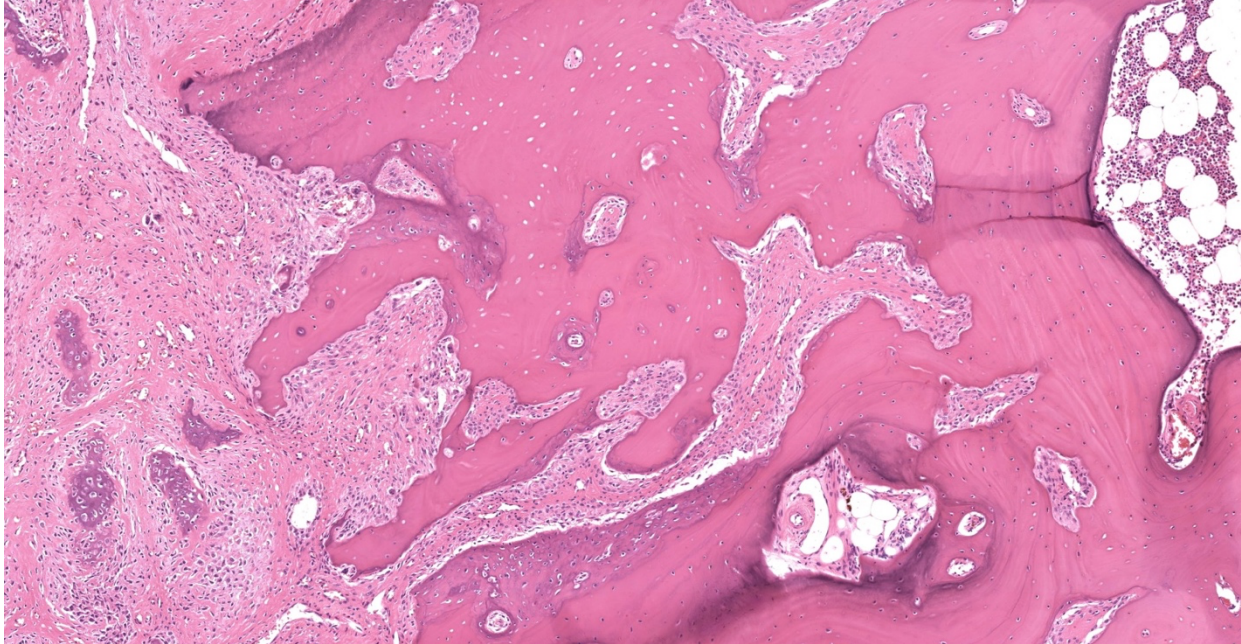
Skull, parietal bone: Multilobular tumor of bone

**Contributor's comment:**

Multilobular tumor of bone (MTB, also known as multilobular osteochondrosarcoma, chondroma rodens, canine multilobular osteoma and chondroma, and calcifying aponeurotic fibroma) is an uncommon neoplasm that occurs most frequently in medium to large breed dogs, though it has also been reported in cats,<sup>1,7</sup> a horse,<sup>6</sup> and a ferret.<sup>3</sup> Almost all MTB arise from the flat bones of the skull, but tumors arising from the chest have also been reported.<sup>5,7</sup> MTB is typically slow-growing but locally invasive, and despite anecdotal reports of low metastatic potential, metastases were identified in 56% of cases in one study<sup>2</sup>, predominantly distributed within the lung, bone and soft tissues. Local recurrence is also common following excision.

MTB typically presents as a hard, well-defined and irregular nodule that arise from the external or internal surface of the skull, with a heterogenous gritty texture on incision that has been described as reminiscent of popcorn balls.<sup>2</sup> The gross appearance is often suggestive of MTB, but differential diagnoses include osteoma, osteosarcoma, chondroma, chondrosarcoma, osteochondroma, osteochondromatosis, ossifying fibroma, meningioma, and craniomandibular osteopathy. The histological appearance of MTB is distinctive, characterized by a mosaic of well-differentiated mineralized and unmineralized cartilaginous and osseous tissue organized into discrete lobules separated by septa of fibrous connective tissue. A three-tier grading system has been developed for MTB<sup>8</sup> based on the criteria of marginal invasion, lobular size, tissue organization, mitotic rate, cellular pleomorphism, and presence of necrosis. Grade III tumors were associated with faster metastasis and local recurrence following excision, as well as shorter survival time.

The tumor in this case was identified as an incidental finding, with the animal's clinical presentation relating to renal failure. Histological assessment of the kidneys identified severe chronic membranomesangial glomerulonephritis



Flat bone, dog. In areas of cortical infiltration, the lobules of cartilage and bone are lost. (HE, 33X)

with interstitial fibrosis and acute renal papillary necrosis, potentially caused by NSAID therapy.

**Contributing Institution:**

Faculty of Veterinary and Agricultural Sciences,  
The University of Melbourne, Werribee,  
Victoria, Australia  
<http://fvas.unimelb.edu.au>

**JPC diagnosis:**

Flat bone: Multilobular tumor of bone.

**JPC comment:**

As indicated by the contributor, multilobular tumor of bone is the preferred nomenclature, and these neoplasms may be either benign or malignant. The precise histogenesis of this neoplasm is yet to be determined, but research has provided a few clues. Most reported multilobular tumors of bone arise from either dermatocranium or viscerocranium, both of which are of intramembranous origin. Calvarial periosteal cambium cells grown in cell cultures have chondrogenic potential and may be the source of these tumors. There is also some evidence that the periosteal cambium layer of the calvarium has a different regulation mechanism than cambium cells in the axial and appendicular skeletal bones.<sup>9</sup>

Typical features of these neoplasms include irregular islands of hypercellular, disorganized bone with bland morphology. An outer fibrous septum surrounds an inner cambium-like cell layer, with a central core of cartilage and/or bone. They often have a gritty, nodular texture, and are well circumscribed. They are most often locally aggressive and invasive, with, as the contributor states, ~56% metastatic rate. When discovered, most metastatic disease is located in lung, bone, and soft tissue.

A recently described case of multilobular tumor of bone in a guinea pig was the first reported occurrence in a rodent. Similar to previously reported cases in other species, the affected guinea pig had an exophytic mass arising from the frontal bone, maxilla, and nasal bone. CT was performed to assist in determining surgical margins, which should be considered prior to antemortem surgical excision.<sup>4</sup>

**References:**

1. Bender S, Blazejewski S, Sánchez M: Diagnostic Imaging in Veterinary Dental Practice. *Journal of the American Veterinary Medical Association* 2014;244(6):651-654.
2. Dernell WS, Straw RC, Cooper MF, Powers BE, LaRue SM, Withrow SJ: Multilobular

- osteochondrosarcoma in 39 dogs: 1979-1993. *J Am Anim Hosp Assoc* 1998;34(1):11-18.
3. Hanley C, Gieger T, Frank P: What is your diagnosis? Multilobular osteoma (MLO). *Journal of the American Veterinary Medical Association* 2004;225(11):1665-1666.
  4. Hatai H, Kido N, Ochiai K. Multilobular tumor of bone on the forehead of a guinea pig. *J Vet Diag Invest.* 2020;32(5):747-749.
  5. Hay CW, Roberts R, Latimer K: Multilobular Tumor of Bone at an Unusual Location in the Axilla of a Dog. *Journal of Small Animal Practice* 1994;35(12):633-636.
  6. Richardson DW, Acland HM: Multilobular osteoma (chondroma rodens) in a horse. *J Am Vet Med Assoc* 1983;182(3):289-291.
  7. Rossetti E, Bertolini G, Zotti A: Multilobular tumour of bone of the thoracic wall in a cat. *J Feline Med Surg* 2007;9(3):254-257.
  8. Straw RC, LeCouteur RA, Powers BE, Withrow SJ: Multilobular osteochondrosarcoma of the canine skull: 16 cases (1978-1988). *J Am Vet Med Assoc* 1989;195(12):1764-1769.
  9. Thompson KG, Dittmer KE. Tumors of Bone. In: Meuten DJ, ed. *Tumors in Domestic Animals*, 5<sup>th</sup> Ed. Ames, IA:John Wiley & Sons, Inc. 2017:409.